

## 18A.1 THE CANOPY HORIZONTAL ARRAY TURBULENCE STUDY (CHATS)

Edward G. Patton<sup>1\*</sup>, Thomas W. Horst<sup>1</sup>, Donald H. Lenschow<sup>1</sup>, Peter P. Sullivan<sup>1</sup>, Steven Oncley<sup>1</sup>, Sean Burns<sup>1</sup>, Alex Guenther<sup>1</sup>, Andreas Held<sup>1</sup>, Thomas Karl<sup>1</sup>, Shane Mayor<sup>1</sup>, Luciana Rizzo<sup>1</sup>, Scott Spuler<sup>1</sup>, Jielun Sun<sup>1</sup>, Andrew Turnipseed<sup>1</sup>, Eugene Allwine<sup>2</sup>, Steven Edburg<sup>2</sup>, Brian Lamb<sup>2</sup>, Roni Avissar<sup>3</sup>, Heidi E. Holder<sup>3</sup>, Ron Calhoun<sup>4</sup>, Jan Kleissl<sup>5</sup>, William Massman<sup>6</sup>, Kyaw Tha Paw U<sup>7</sup>, Jeffrey C. Weil<sup>8</sup>

<sup>1</sup>National Center for Atmospheric Research, Boulder, CO

<sup>2</sup>Washington State University, Pullman, WA

<sup>3</sup>Duke University, Durham, NC

<sup>4</sup>Arizona State University, Tempe, AZ

<sup>5</sup>University of California, San Diego, CA

<sup>6</sup>USDA Forest Service, Fort Collins, CO

<sup>7</sup>University of California, Davis, CA

<sup>8</sup>University of Colorado, Boulder, CO

### 1. MOTIVATION

#### 1.1 Turbulent exchange within and above tall vegetation

Turbulence in the planetary boundary layer (PBL) well above the surface has been shown to be independent of the details of the surface roughness. In this region well-quantified similarity relationships work well when characterizing turbulent fluxes (*e.g.*, Raupach, 1979). However, in the near-surface layer which is directly influenced by roughness elements, *i.e.*, the roughness sublayer, turbulence exhibits dramatically varying properties depending on the detailed structure of the roughness elements (Shaw et al., 1974; Raupach, 1981; Raupach et al., 1996). Turbulence in the roughness sublayer is largely responsible for transporting momentum, heat and scalars between the surface and the flow aloft, and is directly coupled with the overlying larger-scale turbulence. Therefore, accurate characterization of fluxes within the roughness sublayer is crucial for predicting larger-scale atmospheric flow and scalar transport.

Tall plant canopies cover about 30% of the Earth's land surface and are particularly complex roughness structures because of their seasonal variability, flexibility, and porosity. Furthermore, leaves and branches occur in both random and organized distributions within the canopy. Spectra and co-spectra are more sharply peaked for canopy flow than for flow over smooth walls (Shaw et al., 1974; Finnigan, 1979a; Raupach et al., 1986). Near the canopy top, longitudinal and vertical velocity per-

turbations are more strongly correlated than aloft (Raupach, 1981), implying more efficient momentum transport than in the rest of the PBL. Observations have shown that the turbulence here is highly intermittent and dominated in daytime by cool-air downbursts (sweeps) (Finnigan, 1979b; Shaw et al., 1983; Denmead and Bradley, 1985; Baldocchi and Meyers, 1988). Gao et al. (1989) documented the sloping sharp interface between the rising warm air from the canopy (ejections) and sweeps, and determined that these organized motions are responsible for 60–80% of the fluxes of momentum, energy and scalars within and above the canopy. Raupach et al. (1996) postulated that these structures might be roll vortices generated by the shear induced by the drag of the plant canopy.

The ground and the vegetation may serve as either a scalar source or sink; sometimes one may be a source and the other a sink. Species can also chemically react on time scales that affect their transport within and above the canopy (Patton et al., 2001). The distribution of canopy sources/sinks depends on the amount and state of the canopy foliage, which varies throughout the seasonal cycle for deciduous trees; from bare limbs in winter (no photosynthesis and an open canopy) to rapid growth in spring (increasing photosynthesis and canopy density), to maturity in summer (more constant photosynthesis and canopy density), to senescence and leaf-drop in fall (decreasing photosynthesis and canopy density). Thus, a broad spectrum of different conditions occurs through the year, and both dynamical and scalar fluxes exhibit height dependence and seasonal variability.

\*Corresponding address: Edward G. Patton, National Center for Atmospheric Research, P. O. Box 3000, Boulder, CO, 80307-3000. E-mail: patton@ucar.edu

## 1.2 Linking models and measurements

Large-eddy simulation (LES) is one of the best available tools capable of linking turbulent motions with scales ranging from the microscale to the mesoscale. Using a three-dimensional grid, LES solves the time-dependent filtered Navier-Stokes equations to predict all resolved scales of motion as they evolve in space and time while using a subfilter-scale (SFS) model to parameterize only the smallest scales. An important component of LES is that active, passive and reactive scalars can all be incorporated depending on the topic of interest. As numerical techniques and computational capabilities have improved over the last thirty years, LES results have become a direct counterpart to measurements.

An intriguing aspect of canopy-resolving LES is that because of the canopy-imposed length scale (*i.e.*, the canopy height) increased grid resolution can improve the accuracy of the simulation. Whereas increased resolution in simulations over bare ground continually reduces the scale of the peak in the vertical velocity energy spectrum.

## 1.3 Previous SFS campaigns

Despite its myriad contributions to understanding turbulent flows, LES does have shortcomings and needs to be validated and improved to deal with complex flows, especially for surface layers where dependence on the SFS model increases. To address this issue, NCAR in collaboration with several university groups recently carried out two pioneering observational studies to improve subfilter-scale parameterizations over flat terrain with sparse low-lying vegetation (Horizontal Array Turbulence Study, HATS) and over the ocean (Ocean HATS; OHATS) (*e.g.*, Sullivan et al., 2003, Horst et al., 2004). These studies applied a technique first proposed by Tong et al. (1998) that uses horizontal arrays of 14 to 18 sonic anemometers/thermometers deployed at two levels to measure spatially filtered variables and their gradients which appear in the equations of motion. These datasets have provided an observational basis for validating and developing closure approximations.

## 1.4 Canopy influence on SFS motions

Vegetation dramatically complicates the effects of SFS motions. Canopy elements are distributed spatially, thereby spreading sources/sinks of momentum and scalars throughout the canopy layer. The elements also tend to occur in clumps. Large-scale turbulence (larger than the scale of the clumping) interacting with these clumped elements can rapidly break down into smaller wake-scale motions thereby short-circuiting the inertial energy cascade. In addition, depending on the density of

the canopy elements, the spatially-distributed plant structures intercept (and are heated by) solar radiation during daytime and radiatively cool faster than the surface at night. As a result, in daytime (nighttime) they can create stable (unstable) conditions within and beneath the canopy when the overlying atmosphere is unstably (stably) stratified.

To parameterize SFS fluxes, canopy-LES currently assumes that the SFS motions occur within the inertial subrange and that all wake-scale motions are at a small enough scale that they immediately dissipate to heat. Recently, Shaw and Patton (2003) attempted to improve SFS parameterizations for canopy-resolving LES by allowing wake-scale motions to transport turbulence, but in this study the inertial range assumptions were still required. Finnigan (2000) presented an alternative to Kolmogorov's inertial range theory describing the cascade of energy from large to small scales which includes pressure and viscous drag effects of plants, but this theory has not been thoroughly tested. At this point, we do not know the character of within-canopy SFS motions, nor the role played by eddies shed in the lee of the plant elements, nor how these wake-scale motions affect scalar and momentum transport. We hypothesize that spatial variations of the canopy elements modify SFS motions through canopy-induced stratification and scalar/momentum source/sink distributions.

When this experiment was originally proposed, measuring arrays of subfilter-scale variables within the canopy had not been previously attempted, mostly because of the daunting technological challenges and the interdisciplinary nature of the research. However, recently, Zhu et al. (2007) reported an attempt to measure SFS momentum fluxes in a wind-tunnel model canopy using laser-Doppler velocimetry. Their results lend to the importance of this work, but are lacking in the ability to assess the impact of vegetation on scalar transport and to characterize the impact of the large atmospheric boundary layer scales of motion and thermal stratification.

Ultimately, CHATS aims to learn about SFS motions within canopies and thereby improve the coupling between canopy-LES and PBL models. This is an important step in carrying out LES of scalar and momentum transport in this complex regime, and thus in building a unified model of surface-atmospheric exchange in the framework of global and regional land, atmosphere, and chemical models. We also wanted to collect as complete and high-quality a dataset as necessary to be able to test, evaluate and improve one-dimensional column models of coupled land-surface/atmosphere exchange.

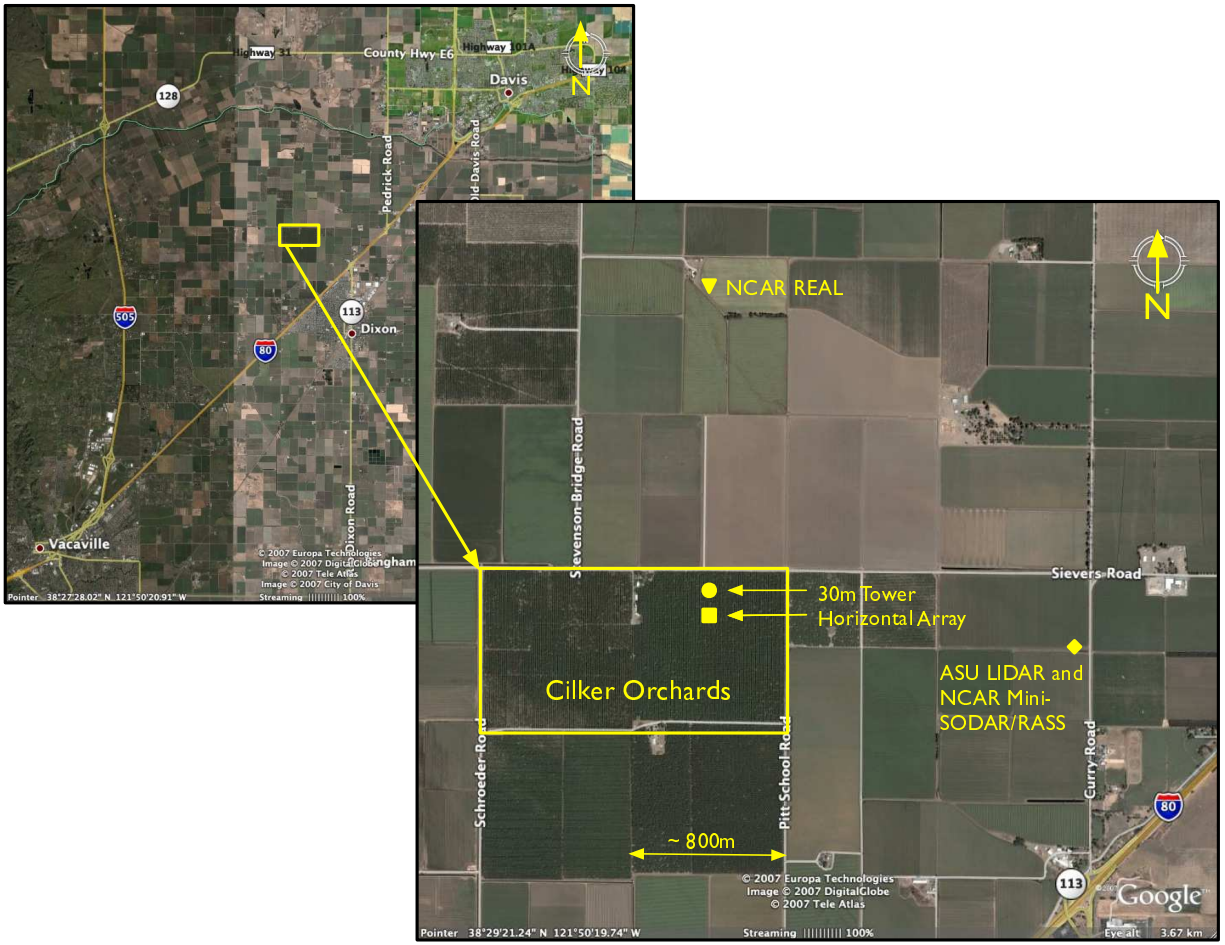


Figure 1: Images from Google Earth depicting the location of Cilker Orchards. Upper left image shows the location of the orchard with respect to Vacaville and Davis, California. Bottom right image shows the location of the various instrumentation with respect to Cilker Orchards.

**2. THE EXPERIMENT**

**2.1 The site**

With the help and equipment largely from NCAR’s In-Situ Sensing Facility, CHATS took place in one of Cilker Orchard’s walnut blocks in Dixon, California (see Figure 1). We chose this location and orchard for many reasons; with the main factors including the size, age, and management practices of the orchard combined with consistent wind direction and speed. Figure 1 shows four 800-m-square sections. As depicted, the CHATS instrumentation focused on the north-east section. In this section, the trees were all Chandler walnuts. To the south is a mix of slightly younger Chandler and Tulare walnuts. To the west is a section of mostly Howard walnuts with a small section of Tulare in the very north-west corner. The section to the south-west is a variety of almonds.

The terrain in this part of California’s Central Valley is flat; less than a 1 m elevation difference across the 1.6 km<sup>2</sup> orchard block. The elevation at the center of the orchard is about 21 m above sea level.

Twenty-four years of data from the Davis California Irrigation Management Information System (CIMIS, <http://www.cimis.water.ca.gov>) showed the mean wind direction to be fairly consistent; 50% from the north and 50% from the south with a small westerly component. We chose to focus on winds from the south because the CIMIS data also showed that winds from the south tend to be weaker in magnitude with smaller direction variability, providing the potential for sampling a greater range of stability. For maximum fetch, the main towers were located near the northern-most border of the section (see Figure 1).

The campaign took place over twelve weeks which was broken into three four-week periods. Intensive mea-

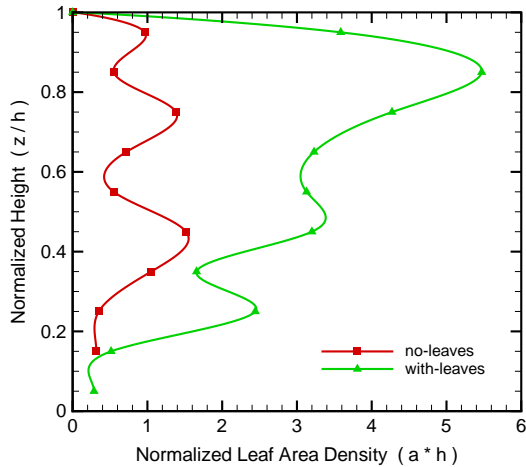


Figure 2: Plant area density profiles measured during CHATS. These profiles are averaged over measurements taken throughout each month of intensive operation and are normalized by the canopy height ( $h$ ). The symbols represent the data, and the lines are parabolic-spline fits. No-leaves: red line with square symbols, With-leaves: green line with triangles.

measurements occurred during first four-week period (March 15 - April 13) focusing on the walnut trees before leaf-out. Measurements continued through the second four-week period (April 14 - May 13), but the instruments were unattended while waiting for the leaves. Intensive measurements then continued during the third four-week period (May 13 - June 12) focusing on the impact of the leaves on the fluid mechanics, stability, and source-sink distribution of the scalars.

The trees in our section were planted in a nearly-square pattern such that they were about 6.9 m apart in the N-S direction, and 7.3 m in the W-E direction. The trees were all about 25 years old with an average height ( $h$ ) of about ten meters. The horizontal distribution of the vegetation was nearly homogeneous with the exception of an occasional tree that had been lost and re-planted. The vertical plant area density distribution was measured regularly through the campaign using a Li-Cor LAI-2000. Before leaf-out, the plant area index (PAI) was about 0.7, while following leaf-out the PAI increased to about 2.5. Figure 2 shows the average vertical profile of normalized plant area density both before and after leaf-out.

## 2.2 Characterizing the canopy-scales and smaller

Within the orchard, the instrumentation was located in two main arrangements. Both the horizontal array and

the thirty meter tower were centered within the section in the W-E direction; the 30 m tower was located about 100 m south from the northern-most edge of the section, and the horizontal array another 100 m south from the tower.

### 2.2.1 The horizontal array

**The towers** The horizontal array consisted of five 12 m tall towers that were deployed in the W-E direction (across the mean wind). The towers were situated such that the three middle towers were each 1.72 m apart with the middle tower situated immediately within the tree row. The outer two towers were located due west or east in the adjacent tree rows, about 7 m away. Therefore, the entire array spanned three tree rows (two row middles).

On each of the four outermost towers, rails were attached to allow a cart to move vertically on the towers. Two carts were designed and manufactured by the NCAR Earth Observing Facility's Design and Fabrication Services. Each of these carts consisted basically of end pieces connecting two horizontal tower sections that were separated vertically by one meter. The carts were attached to ropes and pulleys allowing the carts to be easily raised or lowered to any location from the ground up to the canopy-top or just above. This flexibility facilitated rapid modification of the instrument arrangement with minimal impact on normal orchard operations.

**The main instrumentation** The instrumentation in the horizontal array consisted largely of two rows of sensors vertically separated by one meter. The bottom row included nine CSAT-3 sonic anemometers and five Li-Cor 7500 CO<sub>2</sub>/H<sub>2</sub>O sensors. The 7500's were co-located with the central five CSAT-3's. The top row also included nine CSAT-3 sonic anemometers, but were complemented by five Krypton hygrometers that were also collocated with the central five sonic anemometers. Also set within the upper five central CSAT-3's were five Dantek single-wire hot-film anemometers. These instruments were all oriented toward the south on 1.5m booms.

Due to the difficulties in obtaining accurate mean temperature measurements from the sonic anemometers, two NCAR-Vaisala Hygrothermometers (TRH) collected mean aspirated temperature and relative humidity at 2 Hz; one at each level of the array.

**The scientific plan** During the experiment, the array was modified once every five to seven days. These transitions included cart height and horizontal sensor separation variations. To properly characterize the impact of leaves on the turbulent momentum and scalar fluxes, we repeated each arrangement during the two phases of the experiment (*i.e.*, no-leaves and with-leaves).

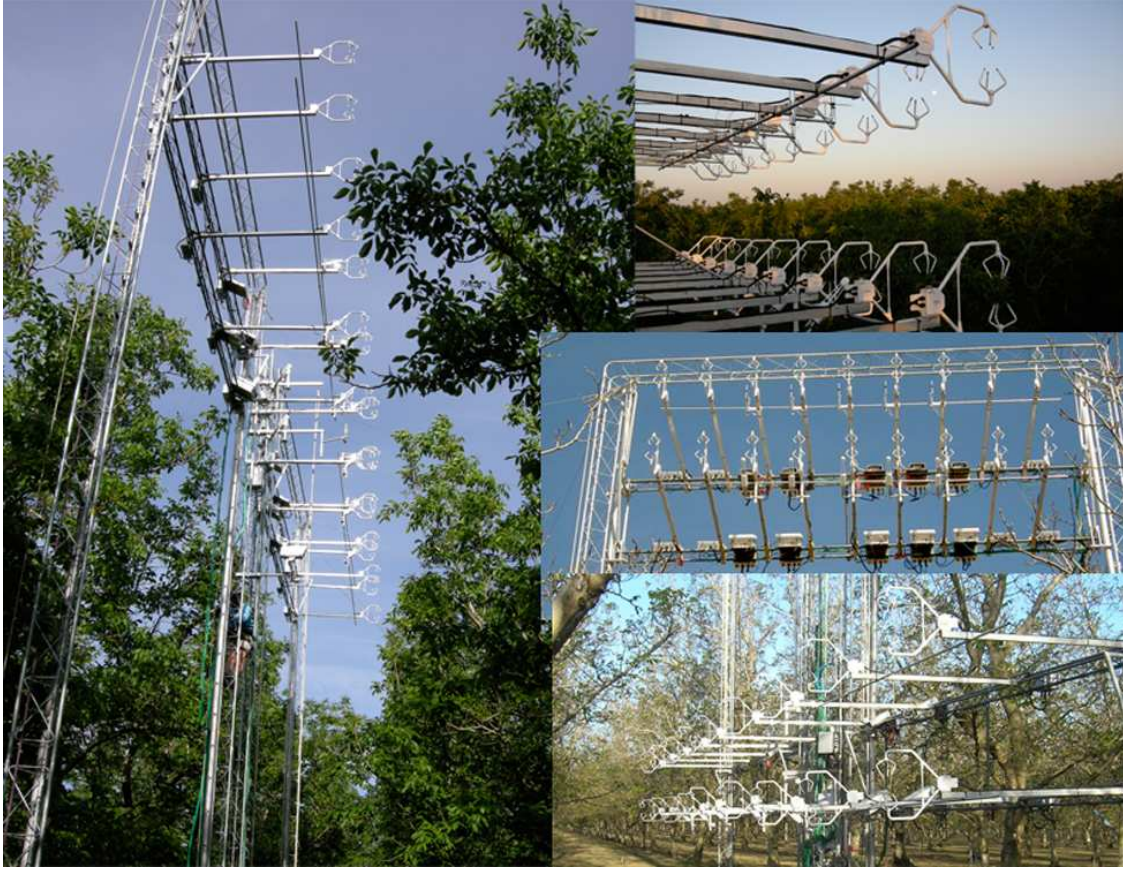


Figure 3: Pictures of the array in CHATS. Left: wide-high arrangement with-leaves; upper-right: narrow-high arrangement with-leaves; middle-right: wide-high arrangement no-leaves, bottom-right: wide-low arrangement no-leaves.

The two horizontal sensor distributions included two separations, 0.5 m and 1.72 m. These spacing were chosen such that when using a five-point filter, the filter-scale separating resolved and sub-filter scale motions would fall at 2 and 6.9 m respectively. The 2 m filter-width was chosen because this width is typical of that used in canopy-resolving LES. The 6.9 m spacing was chosen for a number of reasons. The first is that this was the largest we could go given the constraints imposed by the orchard operations and the length of the horizontal tower sections. The second is that the canopy-imposed elevated velocity shear at the top of the vegetation imposes an important length scale on the flow and we wanted to make sure to have at least one filter-width that fell well within the energy-containing range of the turbulence and therefore averaged much of the canopy-induced scales of motion.

In the “narrow” arrangement (0.5 m separation), all the sensors were located on a single cart and therefore the sensors spanned between two tree-rows or across a single row-middle. In the “wide” arrangement (1.72 m separation), four sensors were located on each level of

each cart, and the middle sensors were located on the central tower.

For each of the intensive months, measurements were taken with the instrumentation configured in six arrangements (the narrow and wide horizontal separations at each of three heights; low - 2.5m , middle - 6m, high - 10.1m). The high location was chosen because it is the region of highest vertical shear of the streamwise velocity and where the majority of the momentum is extracted by the canopy. The middle height was chosen as close as possible to the within-canopy streamwise velocity minimum where we expect wake-scale motions to be extremely important in momentum transport and the peak in the canopy-imposed scalar source/sink distribution to occur. The low height was chosen to be deep within the canopy at a height where the momentum transfer was expected to be largely a result of canopy-scale coherent structures and to be counter-gradient (*i.e.*, the velocity gradient is positive upward, centered at about 2.5 m).

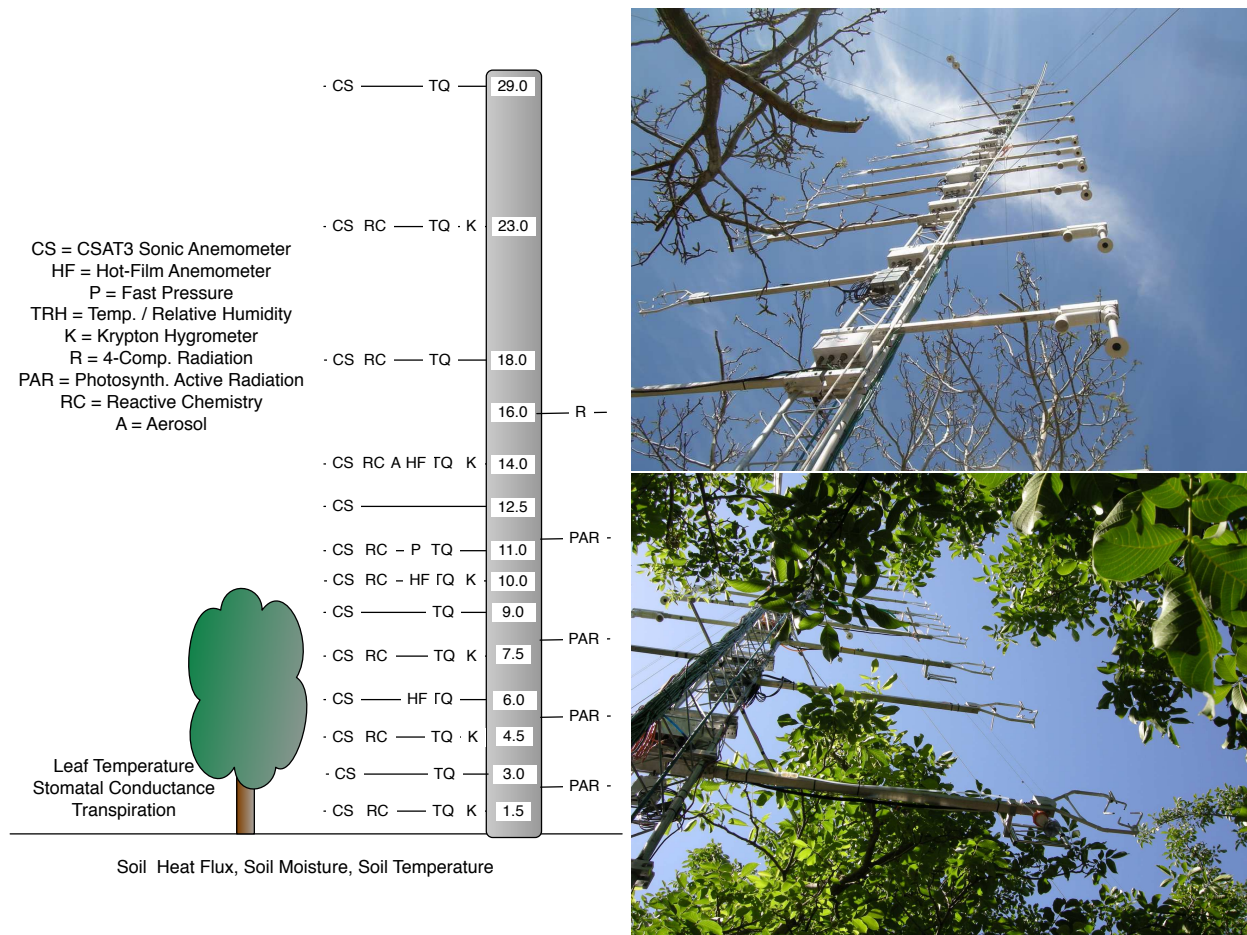


Figure 4: Left: 30 m tower configuration. Numbers on grey tower are in meters. Right: Pictures of the 30m tower from below; above: no-leaves, below: with-leaves.

### 2.2.2 The thirty meter tower

**Velocity, temperature and moisture** The thirty meter tower included thirteen main measurement levels. To accurately capture the turbulence in the high velocity shear region near the canopy top, the instruments were tightly focused about this height and growing in separation distance away from this focal point. Six of these thirteen levels were located below the canopy-top and six above (see Figure 4 for the actual heights). Each of the thirteen primary measurement levels consisted of a Campbell Scientific CSAT-3 sonic anemometer measuring all three wind components and virtual temperature at 60 Hz, and 2) an NCAR-Vaisala Hygrothermometer (TRH) measuring mean aspirated temperature and relative humidity at 2 Hz. At six levels (deployed at every-other level), we sampled specific humidity fluctuations using a Campbell Scientific Krypton hygrometer operating at 20 Hz. To maximize the acceptable wind directions, we deployed the sonic anemometers and the Krypton hygrometers on booms that were 1.5m in length and

directed to the west. To minimize their influence on the turbulence measurements, the TRH's were deployed on similar booms pointing to the east.

Mounted to the center of the sonic anemometers and pointed to the south, we installed a Dantek constant temperature triple-wire hot film anemometer at each of three levels (mid canopy 6m, canopy top 10m, and above canopy 14m) which were sampling at 2 KHz. These sensors will provide direct dissipation measurements as influenced by vegetation.

**Pressure fluctuations** Measurements of turbulent pressure fluctuations ( $p'$ ) were made during CHATS. Quad-disk probes (Nishiyama and Bedard, Jr., 1991) were used to avoid dynamic pressure errors (Figure 5). Ports made by NOAA/ETL were chosen based on wind tunnel testing of three versions of this design. Even these ports have errors that change from below 5% to above 50% as the pitch angle changes from 20 to 30 degrees. Therefore, use of the ports in the canopy (where



Figure 5: Photograph of the quad-disk pressure port when the second pressure port was vertically centered within the array. Also to note in this photograph are the single-wire hot film anemometer mounted within the upper CSAT3 sonic anemometer and the krypton hygrometer located behind.

turbulence intensity and thus instantaneous wind attack angles are large) may require that much of the data be used with caution. One port location was placed in the horizontal array and thus is expected to suffer from this problem, however the other was placed at approximately  $1.1h$ , where Fitzmaurice et al. (2004) found that turbulence intensity has diminished from that found just inside the canopy.

Two types of sensors were used, one similar to that described by Wilczak and Bedard, Jr. (2004) that used an analog transducer and a reference volume with a calibrated leak, and another that used a digital transducer and a fixed reference volume with a large thermal time constant. (A third, slower response, sensor also was deployed to verify the  $p'$  sensor operation at low frequencies.) Before being placed in their final locations, the systems were connected to the same pressure port and determined to be operating properly. Preliminary results indicate that the  $p'$  sensors were responding appropriately.

For the entire second phase of the experiment, one of these pressure ports was shifted into the array. Future work will be to compare these measurements to canopy flow models and to describe the variation of pressure

transport of TKE at the different heights within and near the canopy and to investigate the pressure destruction term in the filtered scalar flux equation that is modeled in LES.

**Radiation** For the entire campaign, a two long- and short-wave Kipp & Zonen radiometers were deployed at 16m to characterize the down-welling and up-welling full-spectrum above-canopy radiation. A similar set of instruments manufactured by Eppley was deployed two tree rows to the west at a height of 2 m to capture the sub-canopy radiational forcing. A Micromet Systems Q7 net radiometer was also installed at this location to complement the Eppley sub-canopy four-component radiation measurements. All radiation measurements were sampled at 1 Hz. Two meters from the sub-canopy radiation measurements, soil moisture, temperature and heat flux were measured at 5cm depth at a rate of 1 Hz.

During the second intensive phase of the experiment, photosynthetically active radiation (PAR) measurements were taken at four heights (2, 5, 8, and 12 m). The uppermost height was a Li-Cor LI-190 Quantum sensor, while the other three levels were Li-Cor LI-191 Line Sensors.

**Reactive chemistry** Most previous studies have assumed negligible chemical effects (either losses or production) upon the measured eddy fluxes of ozone above canopies (for example, see Mikkelsen et al., 2000). However, a recent study implied that up to 50% of the ozone deposition observed may be explained by fast chemistry near or within the canopy between ozone and reactive volatile organic species that are not easily measured (Kurpius and Goldstein, 2003). The large amount of vertical turbulence and flux measurements at CHATS provided an excellent opportunity to study ozone behavior and chemistry throughout a plant canopy.

We combined gradients from vertical profiles of key trace gas species (*e.g.*,  $O_3$ ,  $NO$ ,  $NO_x$ ) measured at (1.5, 4.5, 9, 11, 14, 23)m with disjunct eddy covariance flux measurements of ozone at two levels above the canopy (14 and 23 m) to see if chemistry could be affecting the measured ozone flux.

These trace gas fluxes were taken at similar heights to water vapor fluxes. Because no chemical effects upon  $H_2O$  are expected,  $H_2O$  fluxes serve as a control measurement for deducing vertical divergences in the flux due to factors other than chemistry. For example, during southerly flow across the orchard, we would expect only small vertical divergences in the fluxes of  $H_2O$  and  $O_3$ . However, during periods of northerly winds there is inadequate homogeneous fetch and both  $H_2O$  and  $O_3$  fluxes should exhibit vertical divergences due to differing contributions from the two vegetation types within the flux footprints.

The through-canopy concentration profiles can be combined with the vertical turbulence data to provide further information concerning sources and sinks of these trace gases. To this end, we also measured vertical concentration profiles of CO<sub>2</sub> and H<sub>2</sub>O in order to ascertain the exchange of these passive scalars. These species have similar surface flux controls (*i.e.*, stomata and soil processes) to the more reactive species such as O<sub>3</sub> and NO<sub>x</sub>. We hope that this study serves as a model for our future instrument deployments, integrating fast eddy covariance measurements with canopy profiling in order to better understand within-canopy processes and their impact on measured fluxes.

Gradient measurements of volatile organic compounds (VOC) were performed using a Proton-Transfer-Reaction Mass Spectrometer (PTR-MS\*). On 3 days fast measurements of selected VOCs were performed on 3 levels (4.5m, 9m, 11m). The PTR-MS instrument has a time response (*e.g.*, 10 Hz) suitable for eddy covariance measurements (*e.g.*, 10 Hz, see Karl et al., 2000), and has been used extensively for disjunct eddy covariance measurements (Rinne et al., 2001; Karl et al., 2002; Ammann et al., 2004; Spirig et al., 2005; Lee et al., 2005). Different in-canopy dispersion schemes for various VOCs will be assessed and compared with forward LES model runs to evaluate the emission strength of VOCs emitted by the vegetation.

Surprisingly, and for the first time, high levels (up to 120 pptv) of methyl salicylate [C<sub>6</sub>H<sub>4</sub>(HO)COOCH<sub>3</sub>] were detected in ambient air. PTR-MS mass scans were confirmed by gas chromatograph mass spectrometer (GC-MS) analysis. Profile measurements showed a distinct source of methyl salicylate from the canopy. Methyl salicylate activates specific defense genes through the salicylic acid pathway and is thought to act as a volatile signaling molecule, when plants are under stress or herbivorous attack. In conjunction with detail dispersion analysis available during CHATS these measurements will put constraints on the biological significance of plant to plant communication in the real atmosphere.

**Aerosol measurements - turbulent fluxes and particle size distribution** Particle number concentrations were measured with a condensation particle counter (CPC 3772, TSI Inc., St. Paul, MN) installed on the 30 m tower. The inlet was mounted adjacent to the 14m sonic anemometer. Aerosol data were sampled at 10 Hz with an instrument time constant of 0.43 s. Turbu-

\*PTR-MS employs a soft ionization technique which preserves important information of the measured compound reflected in the corresponding molecular ion. PTR-MS allows for the quantitative on-line detection of VOCs down to pptv-level concentrations (Lindinger et al., 1998; Hansel et al., 1995; de Gouw et al., 2003) without any preceding sample treatment.



Figure 6: A photograph of leaf-level measurements being taken with a Li-Cor 6400 system. A cherry-picker allowed for vertical variations of sunlit- and shaded-leaf exchanges to be documented.

lent aerosol number fluxes will be calculated by direct eddy covariance, and by simulated relaxed eddy accumulation (REA) after investigating the scalar similarity between aerosol particles, sonic temperature, water vapor, and trace gases. If these quantities are transported by eddies similarly efficient throughout the scalar spectra, easily accessible quantities such as sonic temperature may be used as proxy scalars for turbulence parameterizations in future aerosol REA systems, thereby extending current aerosol flux measurement capabilities.

For additional physical characterization (*e.g.* identification of particle formation events, general aerosol burden), particle size distributions were measured in the diameter range from 10 nm to 2  $\mu$ m using a scanning mobility particle sizer (SMPS TSI Inc., St. Paul, MN), a condensation particle counter (CPC 3760 TSI Inc., St. Paul, MN) and an optical particle counter (LASAIR, Particle Measuring Systems, Boulder, CO), sampling below the canopy at 2 m AGL. During the day, aerosol concentrations reached 12,000 particles cm<sup>-3</sup>, decreasing to 3,000 particles cm<sup>-3</sup> at nighttime.

### 2.2.3 Leaf-level measurements

Enclosure systems are used to identify the ecosystem components that control gas and aerosol exchange and develop quantitative parameterizations that can be used in canopy-scale flux models. VOC, CO<sub>2</sub> and H<sub>2</sub>O fluxes from various walnut tree tissues (walnuts, leaves, and stems) were characterized during CHATS using enclosure measurement systems. The systems included a LICOR 6400 leaf cuvette, a 500 ml glass enclosure and a 5 L Teflon bag enclosure. Fluxes of CO<sub>2</sub> and H<sub>2</sub>O were quantified using an infrared gas analyzer. VOC were analyzed using three complementary approaches: 1) the PTR-MS quantified a large range of biogenic VOC, 2) an in-situ GC-MS quantified and identified most of the important biogenic VOC, and 3) samples were collected on solid adsorbent tubes and transported to a highly sensitive laboratory Gas Chromatograph Flame Ionization Detector (GC-FID) system to quantify trace constituents.

The Li-Cor 6400 system, with temperature and light control, was used to investigate the response of VOC, CO<sub>2</sub> and H<sub>2</sub>O fluxes to variations in temperature and light. Individual leaves investigated with this system included shade and sun leaves as well as young and mature leaves (see Figure 6). The glass enclosure was used to examine emissions from undisturbed and wounded walnuts. The Teflon bag enclosure was used to investigate emissions from stems and leaves, including both undisturbed and wounded tissues. Relatively low terpenoid and green leaf volatiles (e.g., hexenol, hexenal) emissions were observed from undisturbed leaves, stems and walnuts. Substantial emissions of green leaf volatiles and dimethyl-nonatriene (DMNT) were observed from wounded leaves. A large number of monoterpenes and sesquiterpenes were emitted from both leaves and walnuts when they were wounded.

### 2.2.4 Infrared Imagery

To measure heat storage in biomass and to determine the boundary conditions for heat exchange between vegetation and soil surfaces and atmosphere a FLIR ThermoCAM SC3000 IR camera was also deployed at the CHATS field site. The camera was mounted atop the horizontal array structure at a height of 12 m looking SSE from to May 12 - June 7, 2007 (not shown). From June 8-10, 2007, it was mounted on a tripod located 5 m South of the center of the array on the ground (this figure) at a height of 167 cm AGL from June 8th to June 10th.

The total heat storage (*S*) in the control volume between soil surface and eddy covariance sensors can be expressed as the sum of heat storage in biomass (trunk and leaves) and air respectively. *S* may be a significant component of the hourly averaged energy balance. In the absence of direct measurements, heat storage in biomass

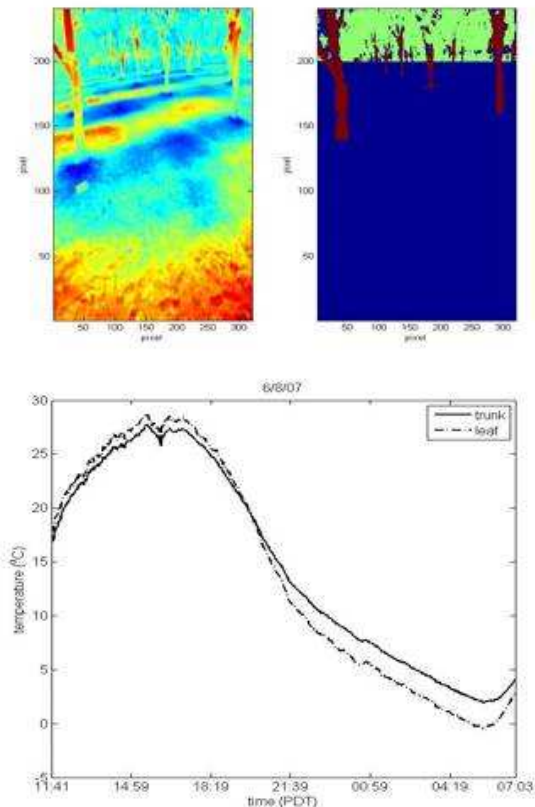


Figure 7: Top: Nighttime IR image on June 8. Bottom: Pixels on the tree trunk (brown) and leaves (green) and soil (blue) as identified. Bottom-right: Time series plot of average leaves and trunk temperature for June 8 - June 9, 2007.

is often approximated by  $S_{veg} = c \times M_{veg} \times \delta T$  where  $M_{veg}$  and  $\delta T$  are mass of the vegetation per unit area and change in representative canopy air temperature (Moore and Fisch, 1986). The constant *c* accounts for the difference in the amplitude of the diurnal temperature cycle between air and canopy and is typically chosen as  $c = 0.8$ . This crude approach produces significant error for energy budgets on short time scales, since canopy temperature lags air temperature by several hours and the different masses and temperatures of trunk, branches, biomass are not considered.

The IR camera measures radiance at 8  $\mu\text{m}$  wavelength and was equipped with a wide-angle lens with a field of view of  $45^\circ \times 60^\circ$  and  $240 \times 320$  pixels. The accuracy of the camera is 1%. Images were acquired every two minutes. Figure 7 shows an IR image and the pixels associated with trunk and leaves as determined using an image processing algorithm. From the images, the diurnal cycle of trunk and leaf surface temperature was obtained (see Figure 7 for an example time series of June 8).

### 2.2.5 Turbulent diffusion measurements; Trace Gas Automated Profiling System (T-GAPS)

To improve our understanding and predictive capability of diffusion in canopy turbulence, a dispersion experiment took place during CHATS. The experiment consisted of a line-source of SF<sub>6</sub> located 40 m upstream of the thirty-meter tower and a meter above the ground, oriented in the E-W direction. Nine syringe samplers placed strategically map out the along-wind surface concentrations. To capture the vertical dispersion, the Washington State University Trace-Gas Automated Profiling System (T-GAPS) continuously sampled from lines on the thirty-meter tower. The T-GAPS system automatically collects and analyzes five-minute averaged whole air samples obtained simultaneously through seven long sample lines. See Benner and Lamb (1985) for additional information about this type of detector system.

## 2.3 Characterizing the canopy-scale, orchard-scales and larger

### 2.3.1 High-resolution aerosol backscatter LIDAR

The NCAR Raman-shifted Eye-safe Aerosol LIDAR (REAL) collected data from March 15 to June 11 from a site 1.6 km directly north of the 30 m tall tower. The instrument is described in detail in a series of papers (Mayor and Spuler, 2004; Spuler and Mayor, 2005; Mayor et al., 2007b). The deployment of REAL at CHATS was aimed to achieve multiple goals including (1) exploration and advancement of the potentially unique ability of the instrument to create time-lapse visualizations of turbulent coherent structures; (2) collect a data set that would allow one to relate changes in the LIDAR aerosol backscatter to several in situ measurements and explore the use of the backscatter data for the remote measurement of 2-point turbulence statistics of scalars; and (3) to characterize the local meso-gamma scale structure of the atmosphere in which the CHATS in situ measurements were made. This includes monitoring boundary layer depth ( $z_i$ ) and deriving the vector flow field via the correlation technique as done previously by Mayor and Eloranta (2001).

REAL is an elastic backscatter LIDAR that operates at a wavelength of 1.5-microns in order to safely transmit high energy laser pulses. This allows it to scan at a sufficient rate to create time-lapse animations of aerosol backscatter that often enable flow visualizations. The LIDAR operated at a pulse rate of 10 Hz and recorded backscatter data in 1.5 meter range intervals. From its location, REAL was able to scan just meters above the canopy. Over 2800 hours of data were collected during its deployment in CHATS. A satellite link allowed scientists to control its operation remotely. Both vertical

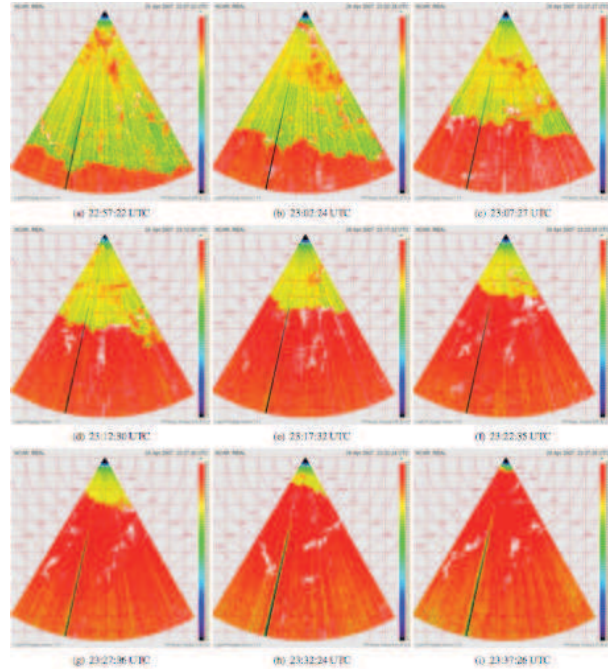


Figure 8: Near-horizontal PPI scans depicting the passage of a sea breeze front passing by the orchard from 22:57:22 UTC to 23:37:26 UTC on 26 April 2007. The elevation angle of the scans is 0.2-degrees above horizontal. Range rings and grid lines are drawn at 500 m intervals. The maximum range shown is 5.8 km. For reference, the noticeable streak in the figures is due to blockage of the laser beam by a tall tree located at a farm house at the northern most edge in the center of the orchard.

and horizontal scans were collected. During periods of southerly winds, the scan strategy was programmed to collect higher angular resolution data around the towers. At other times, wider angle scans were collected. The LIDAR routinely observed good signal to noise aerosol backscatter data to ranges beyond 5 km.

The REAL data set from CHATS contains a number of interesting phenomena including wave propagation and turbulent episodes during stable nocturnal conditions, Kelvin-Helmholtz billow-like structures, dispersion of point sources of particulate matter and area sources of pollen, very shallow mixed layers, and several cases of sea-breeze frontal passages (Figure 8, Mayor et al., 2007a).

### 2.3.2 Coherent Doppler LIDAR

Arizona State University (ASU) deployed its coherent Doppler LIDAR on the second phase of the experiment. The primary motivations of the ASU LIDAR deployment were: 1) to illuminate the connection between the larger-

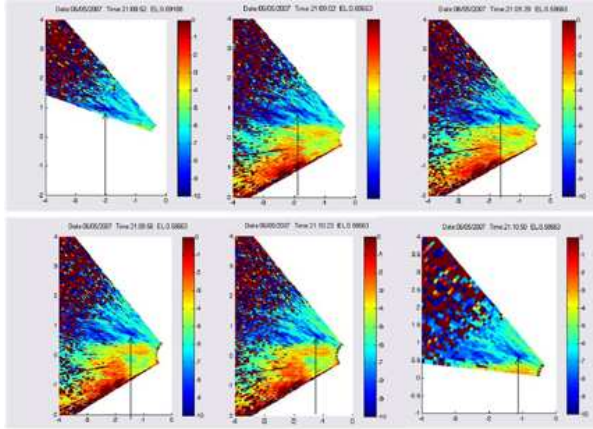


Figure 9: Propagation of a gust during CHATS on 0.58 degree PPI series from the ASU coherent Doppler LIDAR, June 5, 2007. The arrow points to the organized structure.

scales and the canopy flows, 2) to gather Doppler LIDAR data appropriate for 4DVAR analysis, 3) to characterize small-scale winds and turbulence above the canopy, and 4) to measure properties of boundary layer development, such as, the evolution of ABL height and aerosol levels.

The ASU LIDAR was located 2.05 kilometers to the east of the orchard with a clear line of sight (see Figure 1). With an azimuthal angle 279 degrees and an elevation angle of 0.75 degrees, the ASU LIDAR pointed at the top of the 30 m tower.

Generally, the instrument operated well with only limited down periods during the entire second phase of the experiment. Data quality was high and the planned scans for supporting the experiment were executed successfully. Acceptable quality was typically obtained for the LIDAR signal to a range of approximately 4 kilometers, though this varied significantly depending on daily aerosol and humidity levels. Examples of scanning methods were: mixed PPI/RHIs, low-level PPIs for gust tracking, and fast volumetric scans in anticipation of 4DVAR analysis. Some of the latter scans were timed to correspond with a helicopter deployment which took place toward the beginning of the second phase of the experiment.

A preliminary example of the processing of the gathered LIDAR data can be seen in Figure 9 which captures the propagation of a higher momentum wind gust in a sequence of low level PPIs (0.58 degrees). The approximate wind direction is from the west towards the east with a small northerly component. The darker blue patch of radial velocity indicated by the black arrows moves to the east a distance of 900 meters over 120 seconds, corresponding to an advection velocity of 7.5 m/s, which is consistent with the measured radial velocity.

### 2.3.3 Helicopter observation platform (HOP)

The Duke University helicopter observation platform (HOP) also participated in CHATS. HOP consists of a Bell206 Jet Ranger helicopter, which has been equipped with a three-dimensional, high frequency positioning and attitude recording system, a data acquisition and real-time visualization system, and with high-frequency sensors to measure turbulence, temperature, moisture and CO<sub>2</sub> concentration. Thus, it can collect the variables needed to compute the turbulent heat and scalar fluxes (using the eddy-correlation technique) at low altitudes and low airspeeds that are not feasible with airplanes, yet are essential for studying the exchanges between the Earth surface and the atmosphere (Avissar et al., 2008).

During CHATS, HOP flew during four different day time periods. To characterize the large-scale PBL structure, the flight strategy for HOP involved profiling from just above the canopy-top to above the PBL depth in approximately fifty meter increments. At each elevation, samples were taken for about 3km distance. Interspersed with these PBL profiles, HOP flew five W-E horizontal legs sampling at five different N-S locations (one upwind, three over the orchard, and one downwind leg) across the orchard at an elevation of approximately fifteen meters (about five meters above the tree-top). These five legs will provide a mapping of the spatial structure and the evolution across the orchard. Each complete set of samples (PBL profile plus canopy-top mapping) took a little more than an hour. Without refueling, HOP could complete three sets of horizontal passes over the orchard and two PBL profiles. In total, HOP sampled approximately 25 flight hours during CHATS. This data should provide unique insight into the PBL-canopy scale coupling.

### 2.3.4 Mini-SODAR/RASS

To characterize the mean thermal structure and wind field of the PBL during CHATS, NCAR's Metek mini-SODAR/RASS system was deployed about two kilometers to the east of the orchard (see Figure 1). This system operated continuously during the entire three month CHATS campaign.

## 2.4 Education and outreach

About ten undergraduate students and fifteen graduate students from SUNY Stonybrook, U. C. San Diego, U. C. Davis, Arizona State University, and Washington State University were involved in deploying and maintaining some of the instrumentation during CHATS. Three or four groups of graduate students and their advisers from U. C. Berkeley, U. C. Davis, and Sacramento State University visited the site during the experiment. Two un-

dergraduate students from the Atmospheric Science department at U. C. Davis used the CHATS experiment as the subject of a presentation to peers in their turbulence class. A question and answer session took place on site for about thirty third-grade students from an elementary school in Davis, California (and their parents) who visited the site.

An important emphasis of CHATS includes the future availability of the data for the community. The data will be made available via NCAR's Earth Observing Laboratory web site (Currently, <http://www.eol.ucar.edu>). Concerted effort went into designing as complete a program as feasible. We anticipate and hope that many graduate students will be able to utilize the CHATS data in their studies and that the scientific community will find the data useful for improving understanding of canopy-atmosphere exchange.

### 3. Anticipated outcomes

- Determine the impact of vegetation on sub-filter scale momentum/scalar fluxes and dissipation for LES, where the impact of canopy-induced stability is a key aspect. Characterize the pressure destruction term in the scalar flux equation and evaluate subfilter-scale models of this term that is the key sink of scalar flux.
  - Establish the vertical profile of dissipation as influenced by the canopy elements and stability. Determine the impact of vegetation on the relationship between LIDAR-derived turbulence dissipation and that measured directly using the hot-film anemometry.
  - Establish whether pressure correlates with canopy-scale coherent structures like we think; Investigate the linkages between PBL-scale and canopy-scale structure.
  - Investigate the components of heat storage within the canopy and the time-evolution and vertical variation of within-canopy stability
  - Establish horizontal length scales at the canopy-top; Comparisons between helicopter, LIDAR and array data.
  - Investigate canopy and stability influence on turbulent diffusion; validate models.
  - Investigate sub-canopy processing and transport of biogenic reactive species (relate leaf-level to above-canopy fluxes). Test chemical influences on inversion models relating concentration to canopy source/sink distribution.
- Evaluate, test and improve simple models representing coupled canopy-soil-atmosphere exchange in large-scale modeling systems that can not resolve the influence of canopy-induced processes.

### Acknowledgements

First and foremost, we would like to express our sincere gratitude to both the Cilker family and Antonio Paredes. All parties were extremely generous, tolerant and accommodating during CHATS; We really appreciate that they took a sincere interest in the scientific outcome. Their friendly support and cooperation during the experiment was a critical component of the success of the experiment. We look forward to turning the science into practical information for them and the rest of the agricultural community.

Secondly, we would like to acknowledge the extremely skillful, timely, and understanding effort put forward by the NCAR Earth Observing Laboratory field and fabrication staff. The entire crew were a fantastic group to work with and were always willing to put the science first.

We thank Joe Grant from the University of California, Cooperative Extension in Stockton, CA, for his essential role during our search for an appropriate orchard and for ultimately connecting us with the Cilkers.

We thank Jan Hendrickx, New Mexico Tech for loaning the FLIR infrared camera, and Mekonnen Gebremichael, University of Connecticut for loan of one Scintec BLS900. Michael Sankur, Yoichi Shiga, Mandana Farhadieh, Anirban Garai, Dawit Zeweldi, and Erich Uher from U. C. San Diego assisted in the field.

We appreciate Craig Gnos and Roy Gill for allowing us to place research equipment on their property. Both Mario Moratorio and Paul Lum helped establish contact with these farmers and provided advice on instrument location.

We would also like to acknowledge our funding sources that came together to make this program happen. The majority of the support came from two factions of the National Science Foundation; 1) Office of Facilities and Programs and 2) the National Center for Atmospheric Research (NCAR) / Earth Sun Systems Laboratory (ESSL) / The Institute for Integrative Multidisciplinary Earth System Studies (TIIMES) / Biosphere Ecosystem Atmosphere Carbon Hydrology Organics and Nitrogen (BEACHON) program. Other essential support came from the Army Research Office, Arizona State University, Duke University and the University of California.

## REFERENCES

- Ammann, C., C. Spirig, A. Neftel, M. Steinbacher, M. Komenda, and A. Schaub, 2004: Application of PTR-MS for measurements of biogenic VOC in a deciduous forest, *Intl. J. Mass Spectrom.*, **239**, 2-3, 87–101.
- Avissar, R., H. E. Holder, P. Canning, K. Prince, N. Matayashi, R. L. Walko, and K. M. Johnson, 2008: The Duke University helicopter observation platform, *Bull. Amer. Meteorol. Soc.*, **submitted**.
- Baldocchi, D. D. and T. P. Meyers, 1988: Turbulence structure in a deciduous forest, *Boundary-Layer Meteorol.*, **43**, 345–364.
- Benner, R. L. and B. Lamb, 1985: A fast response continuous analyzer for halogenated atmospheric tracers, *J. Atmos. Oceanic Tech.*, **5**, 582–589.
- de Gouw, J. A., P. D. Goldan, C. Warneke, W. C. Kuster, J. M. Roberts, M. Marchewka, S. B. Bertman, A. A. P. Pszenny, and W. C. Keene, 2003: Validation of proton transfer reaction-mass spectrometry (PTR-MS) measurements of gas-phase organic compounds in the atmosphere during the New England Air Quality Study (NEAQS) in 2002, *J. Geophys. Res.*, **108**, D21.
- Denmead, O. T. and E. F. Bradley, 1985: Flux-gradient relationships in a forest canopy, in *The Forest-Atmosphere Interaction*, edited by B. A. Hutchison and B. B. Hicks, pp. 421–442, D. Reidel, Dordrecht.
- Finnigan, J. J., 1979a: Turbulence in waving wheat. I. Mean statistics and honami, *Boundary-Layer Meteorol.*, **16**, 181–211.
- , 1979b: Turbulence in waving wheat. II. Structure of momentum transfer, *Boundary-Layer Meteorol.*, **16**, 213–236.
- , 2000: Turbulence in plant canopies, *Ann. Rev. Fluid Mech.*, **32**, 519–571.
- Fitzmaurice, L., R. H. Shaw, K. T. Paw U, and E. G. Patton, 2004: Three-dimensional scalar microfront systems in a large-eddy simulation of vegetation canopy flow, *Boundary-Layer Meteorol.*, **112**, 107–127.
- Gao, W., R. H. Shaw, and K. T. Paw U, 1989: Observation of organized structure in turbulent flow within and above a forest canopy, *Boundary-Layer Meteorol.*, **47**, 349–377.
- Hansel, A. et al., 1995: Proton transfer reaction mass spectrometry: On-line trace gas analysis at the ppb level, *Intl. J. Mass Spectrom.*, **149-150**, 609–619.
- Horst, T. W., J. Kleissl, D. H. Lenschow, C. Meneveau, C.-H. Moeng, M. B. Parlange, P. P. Sullivan, and J. C. Weil, 2004: HATS: Field observations to obtain spatially filtered turbulence fields from crosswind arrays of sonic anemometers in the atmospheric surface layer, *J. Atmos. Sci.*, **61**, 13, 1566–1581.
- Karl, T., A. Guenther, R. Fall, A. Jordan, and W. Lindinger, 2000: Covariance measurements of methanol, acetaldehyde and other oxygenated VOC fluxes from drying hay using Proton-Transfer-Reaction Mass Spectrometry, *Atmos. Environ.*, **35**, 491–495.
- Karl, T. G., C. Spirig, J. Rinne, C. Stroud, P. Prevost, J. Greenberg, R. Fall, , and A. Guenther, 2002: Virtual disjunct eddy covariance measurements of organic compound fluxes from a subalpine forest using proton transfer reaction mass spectrometry, *Atmos. Chem. Phys.*, **2**, 279–291.
- Kurpius, M. and A. H. Goldstein, 2003: Gas-phase chemistry dominates O<sub>3</sub> loss to a forest, implying a source of aerosols and hydroxyl radicals to the atmosphere, *Geophys. Res. Lett.*, **30**, 7, 1371.
- Lee, A., G. W. Schade, R. Holzinger, and A. H. Goldstein, 2005: A comparison of new measurements of total monoterpene flux with improved measurements of speciated monoterpene flux, *Atmos. Chem. Phys.*, **5**, 505–513.
- Lindinger, W. et al., 1998: Proton-transfer-reaction mass spectrometry (PTR-MS): on-line monitoring of volatile organic compounds at pptv levels, *Chem. Soc. Rev.*, **27**, 5, 347–375.
- Mayor, S. D. and E. W. Eloranta, 2001: Two-dimensional vector wind fields from volume imaging lidar data, *J. Appl. Meteorol.*, **40**, 1331–1346.
- Mayor, S. D. and S. M. Spuler, 2004: Raman-shifted eye-safe aerosol backscatter LIDAR at 1.54 microns, *Appl. Optics*, **43**, 3915–3924.
- Mayor, S. D., S. M. Spuler, B. M. Morley, S. C. Himmelsbach, R. A. Rilling, T. M. Weckwerth, E. G. Patton, and D. H. Lenschow, 2007a: Elastic backscatter lidar observations of sea-breeze fronts in dixon, california, in *7th Amer. Meteorol. Soc. Conf. on Coastal Meteorology*, San Diego, CA.
- Mayor, S. D., S. M. Spuler, B. M. Morley, and E. Loew, 2007b: Polarization LIDAR at 1.54-microns and observations of plumes from aerosol generators, *Opt. Eng.*, **In press**.

- Mikkelsen, T. N., H. Ro-Poulsen, K. Pilegaard, M. F. Hovmand, N. O. Jensen, C. S. Christensen, and P. Hummelshøj, 2000: Ozone uptake by an evergreen forest canopy: Temporal variations and possible mechanisms, *Environ. Pollution*, **109**, 423–429.
- Moore, C. J. and G. Fisch, 1986: Estimating heat storage in amazonian tropical forest, *Agric. For. Meteorol.*, **38**, 147–169.
- Nishiyama, R. T. and A. Bedard, Jr., 1991: A quad-disk static pressure probe for measurement in adverse atmospheres - with a comparative review of static pressure probe designs, *Rev. Sci. Instrum.*, **62**, 2193–2204.
- Patton, E. G., K. J. Davis, M. C. Barth, and P. P. Sullivan, 2001: Decaying scalars emitted by a forest canopy: A numerical study, *Boundary-Layer Meteorol.*, **100**, 91–129.
- Raupach, M. R., 1979: Anomalies in flux-gradient relationships over a forest, *Boundary-Layer Meteorol.*, **16**, 467–486.
- , 1981: Conditional statistics of Reynolds stress in rough-wall and smooth-wall turbulent boundary layers, *J. Fluid Mech.*, **108**, 362–382.
- Raupach, M. R., P. A. Coppin, and B. J. Legg, 1986: Experiments on scalar dispersion within a model plant canopy. Part I: The turbulence structure, *Boundary-Layer Meteorol.*, **35**, 21–52.
- Raupach, M. R., J. J. Finnigan, and Y. Brunet, 1996: Coherent eddies and turbulence in vegetation canopies: The mixing-layer analogy, *Boundary-Layer Meteorol.*, **78**, 351–382.
- Rinne, H. J. I., A. B. Guenther, C. Warneke, J. A. de Gouw, and S. L. Luxembourg, 2001: Disjunct eddy covariance technique for trace gas flux measurements, *Geophys. Res. Lett.*, **28**, **16**, 3139–3142.
- Shaw, R. H. and E. G. Patton, 2003: Canopy element influences on resolved- and subgrid-scale energy within a large-eddy simulation, *Agric. For. Meteorol.*, **115**, 5–17.
- Shaw, R. H., R. H. Silversides, and G. W. Thurtell, 1974: Some observations of turbulent transport within and above plant canopies, *Boundary-Layer Meteorol.*, **5**, 429–449.
- Shaw, R. H., J. Tavangar, and D. P. Ward, 1983: Structure of the Reynolds stress in a canopy layer, *J. Clim. Appl. Meteorol.*, **22**, 1922–1931.
- Spirig, C., A. Neftel, C. Ammann, J. Dommen, W. Grabmer, A. Thielmann, A. Schaub, J. Beauchamp, A. Wisthaler, and A. Hansel, 2005: Eddy covariance flux measurements of biogenic VOCs during ECHO 2003 using proton transfer reaction mass spectrometry, *Atmos. Chem. Phys.*, **5**, **2**, 465–481.
- Spuler, S. M. and S. D. Mayor, 2005: Scanning eye-safe elastic backscatter LIDAR at 1.54 microns, *J. Atmos. Oceanic Tech.*, **22**, 696–703.
- Sullivan, P. P., T. W. Horst, D. H. Lenschow, C.-H. Moeng, and J. C. Weil, 2003: Structure of subfilter-scale fluxes in the atmospheric surface layer with application to large-eddy simulation modelling, *J. Fluid Mech.*, **482**, 101–139.
- Tong, C., J. C. Wyngaard, S. Khanna, and J. G. Brasseur, 1998: Resolvable- and subgrid-scale measurement in the atmospheric surface layer: Technique and issues, *J. Atmos. Sci.*, **55**, 3114–3126.
- Wilczak, J. M. and A. J. Bedard, Jr., 2004: A new turbulence microbarometer and its evaluation using the budget of horizontal heat flux, *J. Atmos. Oceanic Tech.*, **21**, 1170–1181.
- Zhu, W., R. van Hout, and J. Katz, 2007: On the flow structure and turbulence during sweep and ejection events in a wind-tunnel model canopy, *Boundary-Layer Meteorol.*, **124**, 205–233.